Hindawi Publishing Corporation
Mathematical Problems in Engineering
Volume 2010, Article ID 987891, 17 pages
doi:10.1155/2010/987891

Research Article

Weakly Nonlinear Stability Analysis of a Thin Magnetic Fluid during Spin Coating

Cha'o-Kuang Chen and Dong-Yu Lai

Department of Mechanical Engineering, National Cheng Kung University, Tainan 70101, Taiwan

Correspondence should be addressed to Cha'o-Kuang Chen, ckchen@mail.ncku.edu.tw

Received 8 April 2010; Accepted 1 June 2010

Academic Editor: Cristian Toma

This paper investigates the stability of a thin electrically conductive fluid under an applied uniform magnetic filed during spin coating. A generalized nonlinear kinematic model is derived by the long-wave perturbation method to represent the physical system. After linearizing the nonlinear evolution equation, the method of normal mode is applied to study the linear stability. Weakly nonlinear dynamics of film flow is studied by the multiple scales method. The Ginzburg-Landau equation is determined to discuss the necessary conditions of the various critical flow states, namely, subcritical stability, subcritical instability, supercritical stability, and supercritical explosion. The study reveals that the rotation number and the radius of the rotating circular disk generate similar destabilizing effects but the Hartmann number gives a stabilizing effect. Moreover, the optimum conditions can be found to alter stability of the film flow by controlling the applied magnetic field.

1. Introduction

The study of magnetohydrodynamic (MHD) effects is important for a wide range of situations, varying from plasma engineering, MEMS technology, and thin film materials technology. Due to various applications, attention has gradually been focused on this subject [1–12]. In fact, stabilization of the film flow by applying a magnetic field is advantageous as follows: (1) neither electrical nor mechanical contacts with the fluid are necessary; (2) active control of a technological process is simple.

The spin coating process is one of the fundamental fabrication methods found in the chip manufacturing processes of integrated circuit (IC) such as wafer manufacturing, photolithography, and sputtering deposition. Therefore, it is highly desirable to develop suitable working techniques for homogeneous film growth, techniques that are able to adapt to various flow configurations and associated time-dependent properties. For these reasons, the ability to control and maintain uniform and stable thin films is an important research topic with regard to spin coating [13–17].

Linear stability theories for various film flows have been presented by Chandrasekhar [18] and Lin [19]. Stuart [20] was the first to study the weakly nonlinear theory of hydrodynamic stability. This model has been widely employed in subsequent investigations. Long-wave perturbation method is an effective means of revealing the linear and nonlinear evolution equation of the film thickness. The wavelength of surface waves is assumed to be sufficiently large and the perturbation amplitude $\alpha \ll 1$; so the long-wavelength modes that give the smallest wave number are most likely to induce flow instability. Yih [21] indicated that the long-wave perturbation method is appropriate for film flow with a small Reynolds number. Alekseenko et al. [22] investigated the wave formation of a vertical liquid film. The maximum growth rates, wave number, and wave velocities were found theoretically and compared with obtained experimentally at Re $\sim$ 30. Then, the hydrodynamic stability analysis of the thin liquid film by the long-wave perturbation method was performed [23–26]. Furthermore, numerous investigations of hydrodynamic stability have been studied by the experimental observations [27, 28].

Several researchers presented hydromagnetic stability of film flows on a rotating disk [29–32] and the weakly nonlinear analysis of the MHD flow down a vertical plate was published [33]. In this study, the authors present a weakly nonlinear stability analysis of a thin electrically conductive fluid under an applied uniform magnetic field on a rotating disk, namely, spin coating. The induced magnetic field is neglected by assuming that the magnetic Reynolds number $\mathrm{Re}_m \ll 1$ [30] during spin coating. It is also assumed that the disk radius is much larger than the film thickness. Therefore, the peripheral effect is negligible in comparison to the total film area [15]. It is demonstrated that stability is revealed in the region near the rotating axis due to centrifugal forces and MHD effects. The influence of the rotational motion, disk size, and the Hartmann number on the equilibrium finite amplitude is studied and characterized mathematically. In an attempt to verify the computational results and to illustrate the effectiveness of the proposed modeling approach, several numerical examples are presented.

2. Mathematical Formulation

Under the assumption that no polarization voltage is applied (i.e., $\overrightarrow{E} = \overrightarrow{0}$), the electromagnetic force $\overrightarrow{F_m}$ acting on the MHD flow is given:

$$\overrightarrow{F_m} = \overrightarrow{J} \times \overrightarrow{B} = \sigma\left(\overrightarrow{V} \times \overrightarrow{B}\right) \times \overrightarrow{B}, \tag{2.1}$$

where $\overrightarrow{E}$ is the electric field, $\overrightarrow{J}$ the current density, $\overrightarrow{B}$ the magnetic flux, σ the electrical conductivity, and $\overrightarrow{V}$ the velocity vector.

Consider axisymmetric flow of a thin electrically conductive fluid flowing on a rotating circular disk which rotates with constant angular velocity Ω^* under an applied magnetic field B_0^*. The external uniform magnetic field is applied perpendicular to the plane of the disk (see Figure 1). A variable with a superscript "$*$" represents a dimensional quantity. Here the cylindrical polar coordinate axes r^*, θ^*, z^* are chosen as the radial direction, the circumferential direction, and the direction perpendicular to the plate, respectively. All associated physical properties and the rate of film flow are assumed to be constant (i.e., time-invariant) because of the steady mass flow source at the center of rotation. Let u^* and w^* be the velocity components in the radial direction r^* and the perpendicular direction z^*

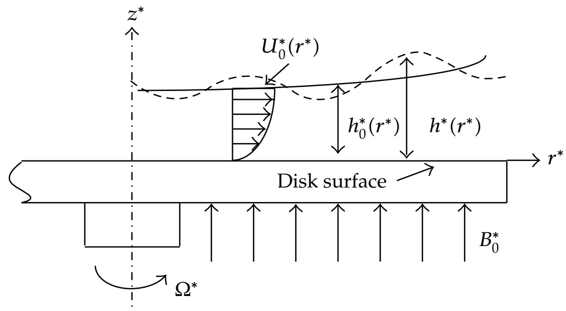

Figure 1: Schematic diagram of a thin MHD fluid flowing on a rotating circular disk.

of a circular disk, respectively. According to the experimental observation by Takama and Kobayashi [34], it is reasonable to assume negligible circumferential flow when the liquid film is very thin ($h^* \ll r^*$). As a matter of simplification, we take the fluid velocity in the thinning film to be independent of θ^*. For small magnetic Reynolds number ($\mathrm{Re}_m \ll 1$), the electromagnetic force F_m is $\sigma B_0^{*2} u^*$ [30, 35], when imposed and induced electric fields are negligible and the only applied magnetic field is B_0^*. The MHD governing equations of motion can be expressed as

$$\frac{1}{r^*}\frac{\partial(r^* u^*)}{\partial r^*}+\frac{\partial w^*}{\partial z^*}=0,$$
$$\rho\left(\frac{\partial u^*}{\partial t^*}+u^*\frac{\partial u^*}{\partial r^*}+w^*\frac{\partial u^*}{\partial z^*}-\frac{v^{*2}}{r^*}\right)=-\frac{\partial p^*}{\partial r^*}+\mu\left(\frac{\partial^2 u^*}{\partial r^{*2}}+\frac{1}{r^*}\frac{\partial u^*}{\partial r^*}+\frac{\partial^2 u^*}{\partial z^{*2}}-\frac{u^*}{r^{*2}}\right)-\sigma B_0^{*2} u^*,$$
$$\frac{\partial w^*}{\partial t^*}+u^*\frac{\partial w^*}{\partial r^*}+w^*\frac{\partial w^*}{\partial z^*}=-\frac{1}{\rho}\frac{\partial p^*}{\partial z^*}-g+\frac{\mu}{\rho}\left(\frac{1}{r^*}\frac{\partial}{\partial r^*}\left(r^*\frac{\partial w^*}{\partial r^*}\right)+\frac{\partial^2 w^*}{\partial z^{*2}}\right), \tag{2.2}$$

where v^* is the azimuthal velocity, ρ the constant fluid density, p^* the fluid pressure, g the acceleration due to gravity, μ the dynamic viscosity of the fluid, and B_0^* is the magnetic flux density.

On the disk surface $z^* = 0$, the boundary conditions are treated as no-slip as

$$u^* = 0,$$
$$w^* = 0. \tag{2.3}$$

On the free surface $z^* = h^*$, the boundary condition approximated by the vanishing of the shear stress is expressed as

$$\left(\frac{\partial u^*}{\partial z^*}+\frac{\partial w^*}{\partial r^*}\right)\left(1-\left(\frac{\partial h^*}{\partial r^*}\right)^2\right)-2^*\left(\frac{\partial u^*}{\partial r^*}-\frac{\partial w^*}{\partial z^*}\right)\left(\frac{\partial h^*}{\partial r^*}\right)=0. \tag{2.4}$$

The normal stress condition obtained by solving the balance equation in the direction normal to the free surface is given as

$$p^* + 2\mu\left(1+\left(\frac{\partial h^*}{\partial r^*}\right)^2\right)^{-1}\left[\frac{\partial h^*}{\partial r^*}\left(\frac{\partial u^*}{\partial z^*}+\frac{\partial w^*}{\partial r^*}\right)-\frac{\partial w^*}{\partial z^*}-\frac{\partial u^*}{\partial r^*}\left(\frac{\partial h^*}{\partial r^*}\right)^2\right]$$
$$+ S^*\frac{\partial^2 h^*}{\partial r^{*2}}\left[1+\left(\frac{\partial h^*}{\partial r^*}\right)^2\right]^{-3/2} = p_a^*. \tag{2.5}$$

The kinematic condition for a material free surface can be given as

$$\frac{\partial h^*}{\partial t^*} + \frac{\partial h^*}{\partial r^*}u^* - w^* = 0, \tag{2.6}$$

where h^* is the local film thickness, S^* is surface tension, and p_a^* is the atmospheric pressure. By introducing a stream function φ^*, the dimensional velocity components can be expressed as

$$u^* = \frac{1}{r^*}\frac{\partial \varphi^*}{\partial z^*}, \qquad w^* = -\frac{1}{r^*}\frac{\partial \varphi^*}{\partial r^*}. \tag{2.7}$$

The following variables are used to form the dimensionless governing equations and boundary conditions

$$z = \frac{z^*}{h_0^*}, \quad r = \frac{\alpha r^*}{h_0^*}, \quad t = \frac{\alpha t^* u_0^*}{h_0^*}, \quad h = \frac{h^*}{h_0^*}, \quad \varphi = \frac{\alpha\varphi^*}{u_0^* h_0^{*2}}, \quad p = \frac{p^* - p_a^*}{\rho u_0^{*2}}, \quad \mathrm{Re} = \frac{u_0^* h_0^*}{\nu},$$
$$\mathrm{Fr} = \frac{g h_0^*}{u_0^{*2}}, \quad S = \frac{S^*}{\rho u_0^{*2} h_0^*}, \quad m = \frac{\sigma B_0^{*2} h_0^{*2}}{\mu}, \quad \alpha = \frac{2\pi h_0^*}{\lambda}, \tag{2.8}$$

where h_0^* is the average film thickness, α the dimensionless wave number, u_0^* the scale of the velocity, ν the kinematic viscosity, Re the Reynolds number, Fr the Froude number, m the Hartmann number, and λ the wavelength.

In order to investigate the effects of angular velocity, Ω^* on the stability of the flow field, it is assumed that the azimuthal velocity is constant [30, 35, 36] throughout the radial direction in the thin film, that is, $v^* = r^*\Omega^*$. The dimensionless parameter Ro (rotation number) is defined as

$$\mathrm{Ro} = \frac{\Omega^* h_0^*}{u_0^*}. \tag{2.9}$$

In terms of these nondimensional variables, the equations of motion can be expressed as

$$r^{-1}\varphi_{zzz} = -\mathrm{Re}\, r\mathrm{Ro}^2 + r^{-1}m\varphi_z + \alpha\,\mathrm{Re}\left(p_r + r^{-1}\varphi_{tz} + r^{-2}\varphi_z\varphi_{rz} - r^{-3}\varphi_z^2 - r^{-2}\varphi_r\varphi_{zz}\right) + O\left(\alpha^2\right),$$
$$p_z = -\mathrm{Fr} + \alpha\left(-\mathrm{Re}^{-1}r^{-1}\varphi_{rzz}\right) + O\left(\alpha^2\right). \tag{2.10}$$

Using the nondimensional variables, the boundary conditions at the surface of the disk $z = 0$ reduce to

$$\varphi = \varphi_r = \varphi_z = 0, \tag{2.11}$$

and the boundary conditions at the free surface of the disk $z = h$ become

$$r^{-1}\varphi_{zz} = \alpha^2\left[r^{-1}\varphi_{rr} - r^{-2}\varphi_r + 2h_r\left(1 - \alpha^2 h_r^2\right)^{-1}\left(2r^{-1}\varphi_{rz} - r^{-2}\varphi_z\right)\right], \tag{2.12}$$

$$p = -S\alpha^2 h_{rr}\left(1 + \alpha^2 h_r^2\right)^{-3/2} + \alpha\left[-2\mathrm{Re}^{-1}\left(1 + \alpha^2 h_r^2\right)^{-1}\left(r^{-1}\varphi_{rz} + r^{-1}\varphi_{zz}h_r\right)\right] + O\left(\alpha^2\right), \tag{2.13}$$

$$h_t + r^{-1}h_r\varphi_z + r^{-1}\varphi_r = 0. \tag{2.14}$$

In practice, the parameter S has a large value and $\alpha \ll 1$; so the term $\alpha^2 S$ is taken to be of order one [33, 37]. Long-wave length modes are considered in the present analysis; this can be done by expanding the stream function and flow pressure in terms of some small wave number ($\alpha \ll 1$) as

$$\varphi = \varphi_0 + \alpha\varphi_1 + O\left(\alpha^2\right),$$
$$p = p_0 + \alpha p_1 + O\left(\alpha^2\right). \tag{2.15}$$

The flow conditions of a film can be obtained by inserting the above expressions into (2.10)–(2.13) and then solving systematically the resulting equations. By collecting all terms of zeroth-order α^0 and first-order α^1 in the above governing equations and boundary conditions, the solutions of the zeroth-order and first-order equations were obtained and are given in Appendix A.

The zeroth-order and first-order solutions are inserted into the dimensionless free surface kinematic equation to yield the following generalized nonlinear kinematic equation:

$$h_t + A(h)h_r + B(h)h_{rr} + C(h)h_{rrr} + D(h)h_{rrrr} + E(h)h_r^2 + F(h)h_r h_{rrr} = 0, \tag{2.16}$$

where $A(h)$, $B(h)$, $C(h)$, $D(h)$, $E(h)$, and $F(h)$ are given in Appendix B. When the Hartmann number m approaches 0, the fluid flow is reduced to the typical Newtonian film flow with no applied magnetic field [38].

3. Stability Analysis

The dimensionless film thickness, when expressed in terms of the perturbed variables, can be given as

$$h(r,t) = 1 + \eta(r,t), \tag{3.1}$$

where η is a perturbed quantity to the stationary film thickness. Substituting the value of $h(r,t)$ into the evolution equation (2.16) and all terms up to order η^3 being collected, the evolution equation of η becomes

$$\begin{aligned}
&\eta_t + A\eta_r + B\eta_{rr} + C\eta_{rrr} + D\eta_{rrrr} + E\eta_r^2 + F\eta_r\eta_{rrr} \\
&\quad = \left(A'\eta + \frac{A''}{2}\eta^2\right)\eta_r + \left(B'\eta + \frac{B''}{2}\eta^2\right)\eta_{rr} \\
&\qquad + \left(C'\eta + \frac{C''}{2}\eta^2\right)\eta_{rrr} + \left(D'\eta + \frac{D''}{2}\eta^2\right)\eta_{rrrr} + (E + E'\eta)\eta_r^2 \\
&\qquad + (F + F'\eta)\eta_r\eta_{rrr} + O\left(\eta^4\right),
\end{aligned} \tag{3.2}$$

where the values of A, B, C, D, E, F and their derivatives are all evaluated at the dimensionless height of the film, $h = 1$.

3.1. *Linear Stability Analysis*

When the nonlinear terms of (3.2) are neglected, the linearized equation is given as

$$\eta_t + A\eta_r + B\eta_{rr} + C\eta_{rrr} + D\eta_{rrrr} = 0. \tag{3.3}$$

In order to use the normal mode analysis, we assume that

$$\eta = a\exp[i(r - dt)] + \text{c.c.}, \tag{3.4}$$

where a is the perturbation amplitude, and c.c. is the complex conjugate counterpart. The complex wave celerity d is given as

$$d = d_r + id_i = (A - C) + i(B - D), \tag{3.5}$$

where d_r and d_i are the linear wave speed and linear growth rate of the disturbance, respectively. The solution of the disturbance about $h(r,t) = 1$ is asymptotically stable or unstable according as $d_i < 0$ or $d_i > 0$. This is equivalent to the inequality $B < D$ or $B > D$.

Table 1: Various states of Landau equation.

Linearly stable (subcritical region) $d_i < 0$	Subcritical instability $E_1 < 0$	$\varepsilon a_0 < (d_i/E_1)^{1/2}$	$a_0 \to 0$	Conditional stability
		$\varepsilon a_0 > (d_i/E_1)^{1/2}$	$a_0 \uparrow$	Subcritical explosive state
	Subcritical (absolute) stability $E_1 > 0$	$a_0 \to 0$		
Linearly unstable (supercritical region) $d_i > 0$	Supercritical explosive state $E_1 < 0$	$a_0 \uparrow$		
	Supercritical stability $E_1 > 0$	$\varepsilon a_0 \to (d_i/E_1)^{1/2}$ $Nc_r \to d_r + d_i(F_1/E_1)$		

3.2. *Weakly Nonlinear Stability Analysis*

Nonlinear effects, when they are sufficiently weak, do not fundamentally alter the nature of the motion. A weakly nonlinear solution can be usefully expressed as weak stability or instability, but the definition is restricted to some neighborhood of critical value [39]. In this paper the authors are interested in investigating the existence of the supercritical and subcritical regions. In order to characterize the weakly nonlinear behavior of the film flows, the method of multiple scales [40] is employed here; as a result, the Ginburg-Landau equation [41] can be derived following the same procedure as in [33] and Cheng and Lin [42]:

$$\frac{\partial a}{\partial t_2} + D_1 \frac{\partial^2 a}{\partial r_1^2} - \varepsilon^{-2} d_i a + (E_1 + iF_1) a^2 \overline{a} = 0, \tag{3.6}$$

where ε is a small perturbation parameter, $t_2 = \varepsilon^2 t,\ r_1 = \varepsilon r$, and

$$\begin{aligned}
e = e_r + i e_i &= \frac{(B' - D' + E - F)(16D - 4B) + 6C(A' - C')}{(16D - 4B)^2 + 36C^2} \\
&\quad + i \frac{6C(B' - D' + E - F) - (A' - C')(16D - 4B)}{(16D - 4B)^2 + 36C^2}, \\
D_1 &= [(B - 6D) + i(3C)], \\
E_1 &= \left(-5B' + 17D' + 4E - 10F\right) e_r - \left(A' - 7C'\right) e_i + \left(-\frac{3}{2} B'' + \frac{3}{2} D'' + E' - F'\right), \\
F_1 &= \left(-5B' + 17D' + 4E - 10F\right) e_i + \left(A' - 7C'\right) e_r + \frac{1}{2}\left(A'' - C''\right).
\end{aligned} \tag{3.7}$$

The overhead bar appearing in (3.6) stands for the complex conjugate of the same variable. Equation (3.6) can be used to investigate the weak nonlinear behavior of the fluid film flow.

In order to solve (3.6), we assume a filtered wave with no spatial modulation; so the filtered wave can be expressed as

$$a = a_0 \exp[-ib(t_2)t_2]. \tag{3.8}$$

After substituting (3.8) into (3.6), one can obtain

$$\frac{\partial a_0}{\partial t_2} = \left(\varepsilon^{-2} d_i - E_1 a_0^2\right) a_0, \tag{3.9}$$

$$\frac{\partial [b(t_2)t_2]}{\partial t_2} = F_1 a_0^2. \tag{3.10}$$

The associated wave amplitude εa_0 in the supercritical stable region is derived and given as

$$\varepsilon a_0 = \sqrt{\frac{d_i}{E_1}}. \tag{3.11}$$

If $E_1 = 0$, then (3.9) is reduced to a linear equation. The second term on the right-hand side of (3.9) is due to the nonlinearity and may moderate or accelerate the exponential growth of the linear disturbance according to the signs of d_i and E_1. Equation (3.10) is used to modify the perturbed wave speed caused by infinitesimal disturbances appearing in the nonlinear system. The Ginzburg-Landau equation can be used to characterize various flow states, with the results summarized in Table 1.

4. Numerical Examples

In order to study the effects of the dimensionless radius, rotation number, and Hartmann number on the stability of a thin flow, we select randomly but within specified ranges physical parameters for the numerical experiments. The ranges for these parameters are based on published reasonable ranges for these parameters [33, 36, 38, 43]. More specifically, these parameters and their values include (1) Reynolds number (range from 0 to 15), (2) dimensionless perturbation wave numbers (range from 0 to 0.12), (3) Rotation number (any one of the three values 0.15, 0.175, and 0.2), (4) dimensionless radius (any one of the three values 10, 15, and 20). (5) Hartman number (any one of the four values 0, 0.05, 0.1, and 0.15). The remaining parameters are treated as constants for all numerical computations since we are considering practical spin coating systems in which these variables are not expected to undergo significant variation. Further, for a simplified analysis, $\alpha^2 S$, Re, and Fr are taken to be of the same order ($\mathbf{O}$ (1)) [34, 38, 43]; so the values of some dimensionless parameters are taken as constants, for example, the dimensionless surface tension $S = 6173.5$ and the Froude number $\mathrm{Fr} = 9.8$.

4.1. Linear Stability Analysis

By setting $d_i = 0$ in the linear stability analysis, the neutral stability curve can be determined easily from (3.5). The $\alpha^2 S$-Re plane is divided into two different characteristic regions by the

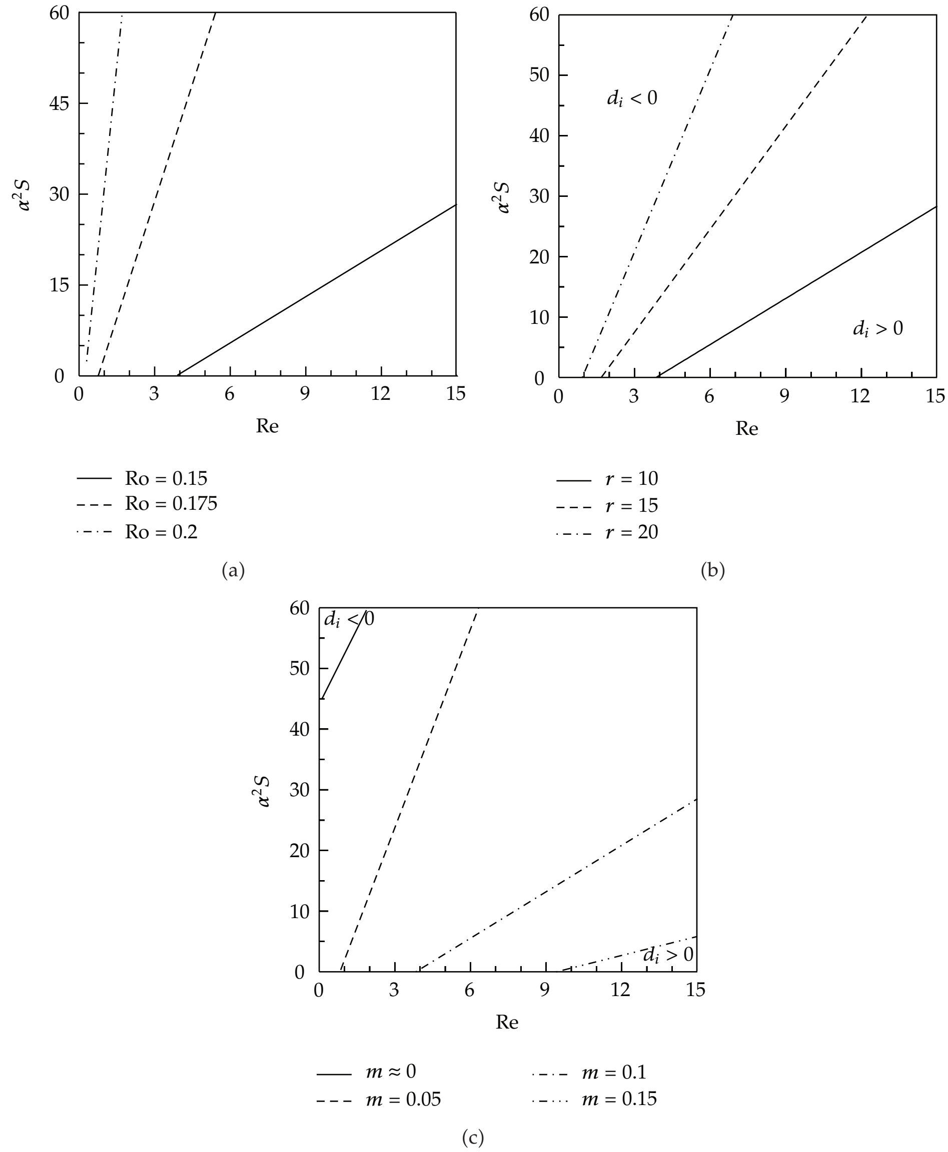

Figure 2: Linear neutral stability curves for three different Ro values at $r = 10$ and $m = 0.1$. Linear neutral stability curves for three different r values at $m = 0.1$ and Ro = 0.1. Linear neutral stability curves for three different m values at $r = 10$ and Ro = 0.1

neutral stability curve. One is the linearly stable region where small disturbances decay with time, and the other is the linearly unstable region where small perturbations grow as time increases. Figure 2(a) shows that the stable region decreases and unstable region increases with an increase of rotation number. Figure 2(b) shows that the stable region decreases and unstable region increases with increasing radius of the circular disk. The reason for this phenomenon is the existence of the centrifugal force term, which is a radius-related force in the governing equation. To increase the radius and the rotation number results in accelerated growth of the linear disturbance due to the centrifugal force. Figure 2(c) shows that the stable

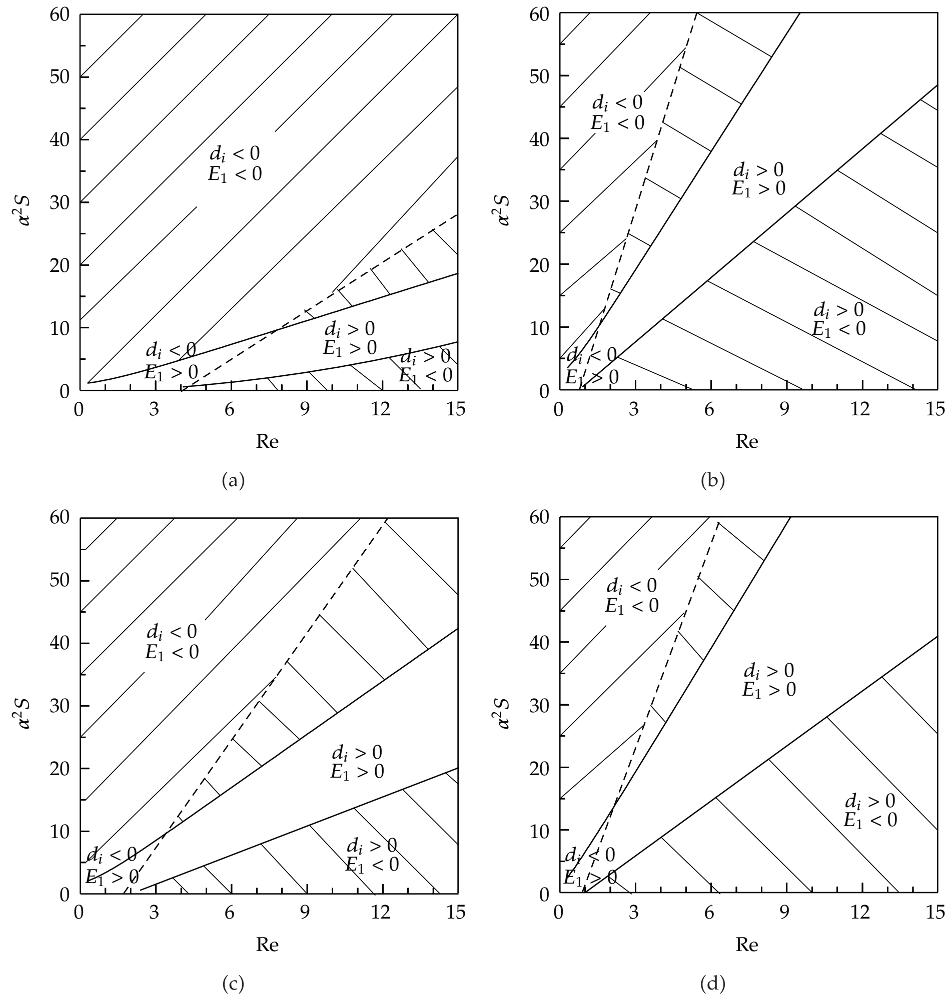

Figure 3: Neutral stability curves of MHD film flows for $r = 10$, Ro = 0.15, and $m = 0.1$. Neutral stability curves of MHD film flows for $r = 10$, Ro = 0.175, and $m = 0.1$. Neutral stability curves of MHD film flows for $r = 15$, Ro = 0.15, and $m = 0.1$. Neutral stability curves of MHD film flows for $r = 10$, Ro = 0.15, and $m = 0.05$

region increases and unstable region decreases with an increase of the Hartman number. The reason for this phenomenon is that the Lorentz forces can modify the velocity field and moderate the growth of linear disturbance. Hence one can say that in linear stability analysis the rotation number and the radius of the circular disk generate similar destabilizing effects but the Hartmann number gives a stabilizing effect.

4.2. Weakly Nonlinear Stability Analysis

Figures 3(a) to 3(d) reveal various conditions for subcritical instability ($d_i < 0, E_1 < 0$), subcritical stability ($d_i < 0, E_1 > 0$), supercritical stability ($d_i > 0, E_1 > 0$) and the supercritical explosion ($d_i > 0, E_1 < 0$). Figure 4(a) shows the threshold amplitude in the sub-critical

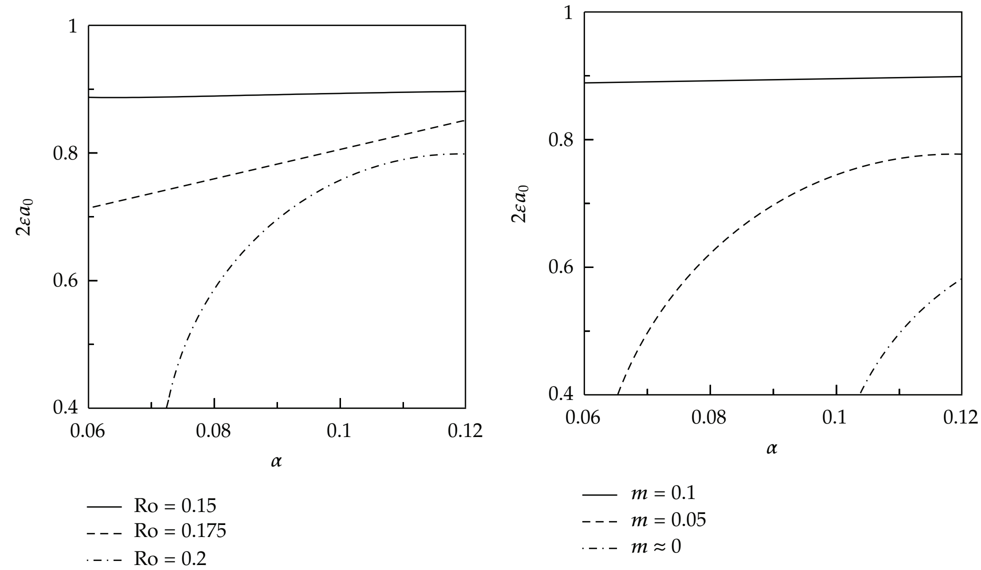

(a) (b)

Figure 4: Threshold amplitude in subcritical instability region for three different Ro values at Re = 3, r = 10, and m = 0.1. Threshold amplitude in subcritical instability region for three different m values at Re = 3, r = 10, and Ro = 0.15

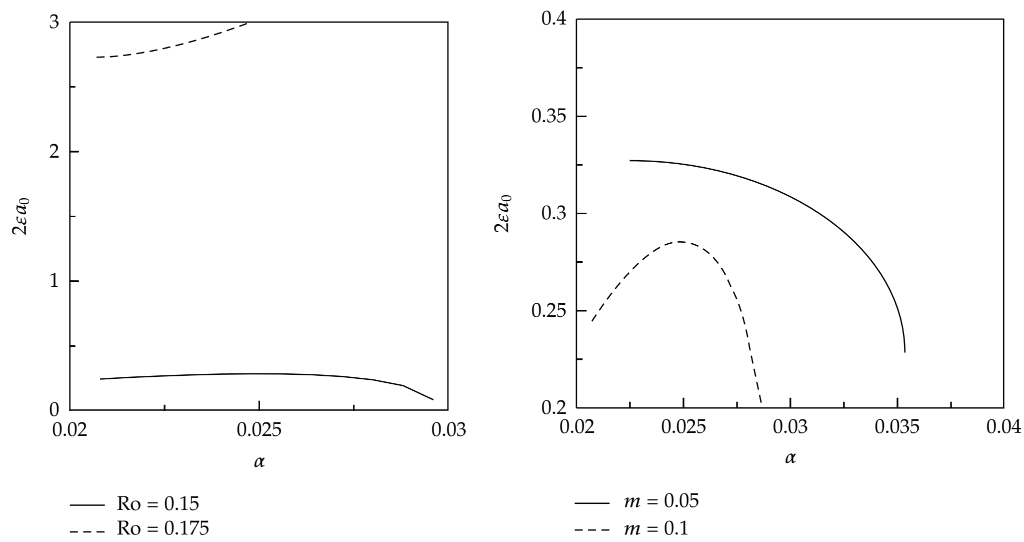

(a) (b)

Figure 5: Threshold amplitude in supercritical stability region for two different Ro values at Re = 6, r = 10 and m = 0.1. Threshold amplitude in supercritical stability region for two different m values at Re = 6, r = 10 and Ro = 0.15

instability region for various wave numbers with different Ro values at Re = 3, r = 10 and m = 0.1. The results indicate that the threshold amplitude εa_0 becomes smaller as the value of the rotation number (Ro) increases. Figure 4(b) shows the threshold amplitude in the sub-critical instability region for various wave numbers with different Hartmann number (m) values at Re = 3, r = 10, and Ro = 0.15. The results indicate that the threshold amplitude εa_0 becomes smaller as the value of m decreases. The film flow which holds the higher threshold amplitude value will become more stable than that holds the smaller one. If the initial finite-amplitude disturbance is less than the threshold amplitude, the system will become conditionally stable.

Figure 5(a) shows the threshold amplitude in the supercritical stability region for various wave numbers with different Ro values at Re = 6, r = 10, and m = 0.1. It is found that decreasing the rotation number will lower the threshold amplitude, whereupon the flow becomes relatively more stable. Figure 5(b) shows the threshold amplitude in the supercritical stability region for various wave numbers with different m values at Re = 6, r = 10 and Ro = 0.15. It is found that increasing the Hartmann number will lower the threshold amplitude, and the flow will become relatively more stable.

5. Concluding Remarks

The stability of a thin electrically conductive fluid under the applied uniform magnetic field during spin coating is investigated using the method of long-wave perturbation. On the basis of the results of numerical modeling, several conclusions can be drawn.

(1) The modeling results indicate that the region of linear stability becomes smaller for increasing rotation number or increasing radius. Hence one can say that in the linear stability analysis the rotation number and the radius of the circular disk generate similar destabilizing effects.

(2) The modeling results also show that the stable region increases and unstable region decreases with an increase of the Hartmann number. In linear stability analysis Hartmann number gives a stabilizing effect.

(3) Weakly nonlinear stability analysis has successfully revealed sub-critical stability, sub-critical instability, supercritical stability, and supercritical explosion regions for the flow patterns of a thin film on a rotating disk under the applied uniform magnetic field. It is found that in sub-critical instability regions, the threshold amplitude εa_0 becomes smaller as the value of the rotation number becomes larger. When the initial finite-amplitude disturbance is less than the threshold amplitude, the flow will be conditionally stable.

(4) It is also shown that in sub-critical instability regions, the threshold amplitude εa_0 becomes larger as the value of the Hartman number becomes larger. Optimum conditions can be obtained: the system is used to increase the stability of the film flow by controlling the applied magnetic field.

Appendices

A. Zeroth-Order and First-Order Solutions

Zeroth-order solution:

$$\varphi_0 = \frac{\mathrm{Re}\cdot r^2\cdot \mathrm{Ro}^2\cdot \mathrm{Sech}(h\sqrt{m})\left[\sqrt{m}\cdot z\cdot \mathrm{Cosh}(h\sqrt{m}) - \mathrm{Sinh}(h\sqrt{m}) + \mathrm{Sinh}((h-z)\sqrt{m})\right]}{m^{3/2}}, \tag{A.1}$$

where the zero-order governing equation:

$$\begin{gathered} r^{-1}\varphi_{0zzz} = -\mathrm{Re}\, r\mathrm{Ro}^2 + r^{-1}m\varphi_{0z}, \\ p_{0z} = -\mathrm{Fr}, \end{gathered} \tag{A.2}$$

associated with boundary condition:

$$\begin{gathered} z=0, \quad \varphi_0 = \varphi_{0z} = 0, \quad z = h, \\ r^{-1}\varphi_{0zz} = 0, \quad p_0 = -\alpha^2 S h_{rr}. \end{gathered} \tag{A.3}$$

First-order solution:

$$\varphi_1 = k_1 z^4 + k_2 z^3 + k_3 z^2 + k_4 z + k_5, \tag{A.4}$$

where

$$\begin{aligned}
k_1 &= -\frac{r^2\cdot \mathrm{Re}\cdot \mathrm{Ro}^4}{12m^2}, \\
k_2 &= \frac{1}{6m^{5/2}} \\
&\quad\times \Big(r\Big(2r\cdot \mathrm{Re}\cdot \mathrm{Ro}^4\Big(\sqrt{m}\Big(1+\mathrm{Sech}(h\sqrt{m})^2\Big) + \mathrm{Tanh}(h\sqrt{m})\Big) \\
&\qquad + \Big(\mathrm{Fr}\cdot m^{5/2} - m\cdot r^2\cdot \mathrm{Re}\cdot \mathrm{Ro}^4\cdot \mathrm{Sech}(h\sqrt{m})^2\cdot \mathrm{Tanh}(h\sqrt{m})\Big)h_r - m^{5/2}S\cdot \alpha^2 h_{rrr}\Big)\Big) \\
k_3 &= \frac{1}{4m^3} \\
&\quad\times \Big(r\Big(-2m^2\cdot r\cdot \mathrm{Re}\cdot \mathrm{Ro}^2\cdot h_{0t}\cdot \mathrm{Sech}(h\sqrt{m}) + r\cdot \mathrm{Re}\cdot \mathrm{Ro}^4 \\
&\qquad\quad \times (2(-2+h)h\cdot m + \mathrm{Sech}(h\sqrt{m}) \\
&\qquad\qquad \times(-4h\cdot m + (1-4h\cdot m)\mathrm{Sech}(h\sqrt{m}) + 4\sqrt{m}(-h+\mathrm{Sech}(h\sqrt{m}))\mathrm{Sinh}(h\sqrt{m}))) \\
&\qquad\qquad -2\Big(\mathrm{Fr}\cdot h\cdot m^3 + m\cdot r^2\cdot \mathrm{Re}\cdot \mathrm{Ro}^4\cdot \mathrm{Sech}(h\sqrt{m})^2 \\
&\qquad\quad \times(-h\sqrt{m} + \mathrm{Sinh}(h\sqrt{m}))\mathrm{Tanh}(h\sqrt{m}))h_r + 2h\cdot m^3\cdot S\cdot \alpha^2 h_{rrr}\Big)\Big)
\end{aligned}$$

$$k_4 = \frac{1}{8m^{7/2}}$$
$$\times \Big(r^2 \cdot \mathrm{Re} \cdot \mathrm{Ro}^4 \cdot \mathrm{Sech}\big(h\sqrt{m}\big)^3$$
$$\times \Big(4\sqrt{m}\Big(13\,\mathrm{Cosh}\big(h\sqrt{m}\big) + 3\,\mathrm{Cosh}\big(3h\sqrt{m}\big) + \mathrm{Cosh}\big(\sqrt{m}(-3h+z)\big)$$
$$+ 2\,\mathrm{Cosh}\big(\sqrt{m}(-h+z)\big) + \mathrm{Cosh}\big(\sqrt{m}(h+z)\big) - \mathrm{Sinh}\big(h\sqrt{m}\big)$$
$$- \mathrm{Sinh}\big(3h\sqrt{m}\big) + 4\,\mathrm{Sinh}\big(\sqrt{m}(-3h+z)\big)$$
$$+2\,\mathrm{Sinh}\big(\sqrt{m}(-h+z) + \mathrm{Sinh}\big(\sqrt{m}(h+z)\big) - 8mr\,\mathrm{Sinh}\big(\sqrt{m}h_r\big)\big)$$
$$\times h_r + 2h \cdot m^3 \cdot S \cdot \alpha^2 h_{rrr}\Big)\Big)\Big)$$

$$k_5 = \frac{1}{16m^4}$$
$$\times \Big(r^2 \cdot \mathrm{Re} \cdot \mathrm{Ro}^4 \cdot \mathrm{Sech}\big(h\sqrt{m}\big)^3$$
$$\times \Big(16m^2\mathrm{Cosh}\big(h\sqrt{m}\big)\mathrm{Cosh}\big(z\sqrt{m}\big)h_{0t} - \mathrm{Ro}^2\mathrm{Cosh}\big(\sqrt{m}(h-2z)\big)$$
$$+ 8\,\mathrm{Cosh}\big(\sqrt{m}(-3h+z)\big) + 32\,\mathrm{Cosh}\big(\sqrt{m}(-h+z)\big)$$
$$+ 24\,\mathrm{Cosh}\sqrt{m}(h+z) + \mathrm{Cosh}\big(\sqrt{m}(-3h+2z)\big)$$
$$+ 16\sqrt{m}(2\,\mathrm{Sinh}\big(\sqrt{m}(-3h+z)\big) + 5\,\mathrm{Sinh}\big(\sqrt{m}(-h+z)\big) + 3\,\mathrm{Sinh}\big(\sqrt{m}(h+z)\big)$$
$$-16m \cdot r \cdot \mathrm{Sinh}\big(h\sqrt{m}\big)\mathrm{Sinh}\big(z\sqrt{m}\big)h_r)\Big)\Big)$$

$$h_{0t} = -\frac{\mathrm{Re} \cdot \mathrm{Ro}^2\Big(2\big(h\sqrt{m} - \mathrm{Tanh}\big(h\sqrt{m}\big)\big) + \sqrt{m} \cdot r \cdot \mathrm{Tanh}\big(h\sqrt{m}\big)^2 h_r\Big)}{m^{3/2}} \tag{A.5}$$

where the first-order governing equation:

$$\begin{gathered} r^{-1}\varphi_{1zzz} = \mathrm{Re}\Big(p_{0r} + r^{-1}\varphi_{0tz} + r^{-2}\varphi_{0z}\varphi_{0rz} - r^{-3}\varphi_{0z}^2 - r^{-2}\varphi_{0r}\varphi_{0zz}\Big), \\ p_{1z} = -\mathrm{Re}^{-1}r^{-1}\varphi_{0rzz}. \end{gathered} \tag{A.6}$$

associated with boundary condition

$$\begin{gathered} z = 0, \quad \varphi_0 = \varphi_{0z} = 0, \quad z = h, \\ r^{-1}\varphi_{1zz} = 0, \quad p_1 = -2\mathrm{Re}^{-1}\Big(r^{-1}\varphi_{0rz} + r^{-1}\varphi_{0zz}h_r\Big). \end{gathered} \tag{A.7}$$

B. Generalized Nonlinear Kinematic Equation

One has

$$\begin{aligned}
A(h) &= \frac{1}{12m^{7/2}r}\operatorname{Sech}\left(h\sqrt{m}\right)^2 \\
&\quad\times\Big(2\sqrt{m}\Big(-3m^2r^2\mathrm{Ro}^2-\mathrm{Fr}\cdot h^3m^3\alpha+30r^2\mathrm{Re}^2\mathrm{Ro}^4\alpha \\
&\qquad\qquad + (h-18)h^2m\cdot r^2\mathrm{Re}^2\mathrm{Ro}^4\alpha \\
&\qquad\qquad + \left(3m^2r^2\mathrm{Ro}^2-\mathrm{Fr}\cdot h^3m^3\alpha+h^2(5h-6)m\cdot r^2\mathrm{Re}^2\mathrm{Ro}^4\alpha\right) \\
&\qquad\qquad \times\operatorname{Cosh}\left(2h\sqrt{m}\right)\Big) - r^2\mathrm{Re}^2\mathrm{Ro}^4\alpha \\
&\qquad \times\left(2h\cdot m(42+h(9-14h\cdot m))-48\operatorname{Cosh}\left(h\sqrt{m}\right)+3\left(1+4h^2m\right)\operatorname{Cosh}\left(h\sqrt{m}\right)\right) \\
&\qquad \times\operatorname{Tanh}\left(h\sqrt{m}\right)\Big), \\
B(h) &= \frac{1}{3}h\cdot\alpha\cdot\mathrm{Re}\left(-\mathrm{Fr}\cdot h^2+\frac{(3-h^2m)r^2\mathrm{Re}^2\cdot\mathrm{Ro}^4\operatorname{Sech}\left(h\sqrt{m}\right)^2\operatorname{Tanh}\left(h\sqrt{m}\right)}{m^{5/2}}\right), \\
C(h) &= \frac{S\cdot\mathrm{Re}\cdot h^3\alpha^3}{3r}, \\
D(h) &= \frac{S\cdot\mathrm{Re}\cdot h^3\alpha^3}{3}, \\
E(h) &= \frac{1}{24m^{5/2}} \\
&\quad\times\Big(\alpha\cdot\operatorname{Sech}\left(h\sqrt{m}\right)^4 \\
&\qquad\times\Big(h\sqrt{m}\Big(-9\,\mathrm{Fr}\cdot h\cdot m^2+16\left(h^2m-3\right)r^2\mathrm{Re}^3\mathrm{Ro}^4 \\
&\qquad\qquad -4\left(3\,\mathrm{Fr}\cdot h\cdot m^2+2\left(h\cdot m^2-3\right)r^2\,\mathrm{Re}\,\mathrm{Ro}^4\right)\operatorname{Cosh}\left(2h\sqrt{m}\right) \\
&\qquad\qquad -3\,\mathrm{Fr}\cdot h\cdot m^2\operatorname{Cosh}\left(4h\sqrt{m}\right)\Big) \\
&\qquad\quad +12\left(h^2m-1\right)r^2\mathrm{Re}^3\mathrm{Ro}^4\operatorname{Sinh}\left(2h\sqrt{m}\right)\Big)\Big), \\
F(h) &= \mathrm{Re}\cdot S\cdot h^2\alpha^3.
\end{aligned}\tag{B.1}$$

Acknowledgment

The authors sincerely thank the reviewer for his useful comments and suggestions which have helped in improving the quality of this manuscript.

References

[1] K. Wasa, M. Kitabatake, and H. Adachi, *Thin Film Materials Technology: Sputtering of Compound Materials*, William Andrew Publishing, New York, NY, USA, 2004.

[2] M. H. Chang and C.-K. Chen, "Hydromagnetic stability of current-induced flow in a small gap between concentric rotating cylinders," *Proceedings of the Royal Society A*, vol. 454, no. 1975, pp. 1857–1873, 1998.

[3] J. Jang and S. S. Lee, “Theoretical and experimental study of MHD (magnetohydrodynamic) micropump,” *Sensors and Actuators A*, vol. 80, no. 1, pp. 84–89, 2000.
[4] G. Herdrich, M. Auweter-Kurtz, M. Fertig, A. Nawaz, and D. Petkow, “MHD flow control for plasma technology applications,” *Vacuum*, vol. 80, no. 11-12, pp. 1167–1173, 2006.
[5] T. Hayat, M. Umar Qureshi, and Q. Hussain, “Effect of heat transfer on the peristaltic flow of an electrically conducting fluid in a porous space,” *Applied Mathematical Modelling*, vol. 33, no. 4, pp. 1862–1873, 2009.
[6] T. Hayat, Q. Hussain, and T. Javed, “The modified decomposition method and Padé approximants for the MHD flow over a non-linear stretching sheet,” *Nonlinear Analysis. Real World Applications*, vol. 10, no. 2, pp. 966–973, 2009.
[7] M. Husain, T. Hayat, and C. Fetecau, “A note on decay of potential vortex in an Oldroyd-B fluid through a porous space,” *Nonlinear Analysis. Real World Application*, vol. 10, no. 4, pp. 2133–2138, 2009.
[8] T. Hayat, T. Javed, and Z. Abbas, “MHD flow of a micropolar fluid near a stagnation-point towards a non-linear stretching surface,” *Nonlinear Analysis. Real World Applications*, vol. 10, no. 3, pp. 1514–1526, 2009.
[9] S. Abbasbandy and T. Hayat, “Solution of the MHD Falkner-Skan flow by homotopy analysis method,” *Communications in Nonlinear Science and Numerical Simulation*, vol. 14, no. 9-10, pp. 3591–3598, 2009.
[10] T. Hayat, Z. Abbas, and M. Sajid, “MHD stagnation-point flow of an upper-convected Maxwell fluid over a stretching surface,” *Chaos, Solitons and Fractals*, vol. 39, no. 2, pp. 840–848, 2009.
[11] S. Abbasbandy and T. Hayat, “Solution of the MHD Falkner-Skan flow by Hankel-Padé method,” *Physics Letters. Section A*, vol. 373, no. 7, pp. 731–734, 2009.
[12] T. Hayat, S. Nadeem, R. Ellahi, and S. Asghar, “The influence of Hall current in a circular duct,” *Nonlinear Analysis. Real World Applications*, vol. 11, no. 1, pp. 184–189, 2010.
[13] A. G. Emslie, F. T. Bonner, and L. G. Peck, “Flow of a viscous liquid on a rotating disk,” vol. 29, pp. 858–862, 1958.
[14] B. G. Higgins, “Film flow on a rotating disk,” *Fluids*, vol. 29, no. 11, pp. 3522–3529, 1986.
[15] A. Kitamura, E. Hasegawa, and M. Yoshizawa, “Asymptotic analysis of the formation of thin liquid film in spin coating,” *Japan Society of Fluid Mechanics*, vol. 30, no. 2, pp. 107–125, 2002.
[16] Y.-K. Yang and T.-C. Chang, “Experimental analysis and optimization of a photo resist coating process for photolithography in wafer fabrication,” *Microelectronics Journal*, vol. 37, no. 8, pp. 746–751, 2006.
[17] Y. K. Kuo and C. G. Chao, “Control ability of spin coating planarization of resist film and optimal of developers,” *Microelectronics*, vol. 37, p. 759, 2006.
[18] S. Chandrasekhar, *Hydrodynamic and Hydromagnetic Stability*, The International Series of Monographs on Physics, Oxford University Press, New York, NY, USA, 1961.
[19] C. C. Lin, *The Theory of Hydrodynamic Stability*, Cambridge University Press, Cambridge, UK, 1955.
[20] J. T. Stuart, “On the role of Reynolds stresses in stability theory,” *Journal of Aerospace Science and Technologies*, vol. 23, pp. 86–88, 1956.
[21] C.-S. Yih, “Stability of liquid flow down an inclined plane,” *Physics of Fluids*, vol. 6, no. 3, pp. 321–334, 1963.
[22] S. V. Alekseenko, V. Ye. Nakoryakov, and B. G. Pokusaev, “Wave formation on a vertical falling liquid film,” *AIChE Journal*, vol. 31, no. 9, pp. 1446–1460, 1985.
[23] D. J. Benney, “Long waves on liquid films,” *Journal of Mathematical Physics*, vol. 45, pp. 150–155, 1966.
[24] B. Gjevik, “Occurrence of finite-amplitude surface waves on falling liquid films,” *Physics of Fluids*, vol. 13, no. 8, pp. 1918–1925, 1970.
[25] S. Korsunsky, “Long waves on a thin layer of conducting fluid flowing down an inclined plane in an electromagnetic field,” *European Journal of Mechanics B*, vol. 18, no. 2, pp. 295–313, 1999.
[26] A. Samanta, “Stability of liquid film falling down a vertical non-uniformly heated wall,” *Physica D*, vol. 237, no. 20, pp. 2587–2598, 2008.
[27] A. Kudrolli, B. Pier, and J. P. Gollub, “Superlattice patterns in surface waves,” *Physica D*, vol. 123, no. 1–4, pp. 99–111, 1998.
[28] S. V. Alekseenjo and D. M. Markkovich, “Jet flow in a bank of cylinders,” *Previews of Heat and Mass Transfer*, vol. 21, no. 4, pp. 302–312, 1995.
[29] E. R. Benton and D. E. Loper, “On the spin-up of an electrically conducting fluid,” *The Journal of Fluid Mechanics*, vol. 39, pp. 561–586, 1969.
[30] H. A. Attia, “Unsteady MHD flow near a rotating porous disk with uniform suction or injection,” *Fluid Dynamics Research*, vol. 23, no. 5, pp. 283–290, 1998.

[31] K. D. Singh, "An oscillatory hydromagnetic Couette flow in a rotating system," *ZAMM Zeitschrift fur Angewandte Mathematik und Mechanik*, vol. 80, no. 6, pp. 429–432, 2000.
[32] S. Asghar, S. B. Khan, A. M. Siddiqui, and T. Hayat, "Exact solutions for magnetohydrodynamic flow in a rotating fluid," *Acta Mechanica Sinica*, vol. 18, no. 3, pp. 244–251, 2002.
[33] J.-S. Tsai, C.-I. Hung, and C.-K. Chen, "Nonlinear hydromagnetic stability analysis of condensation film flow down a vertical plate," *Acta Mechanica*, vol. 118, pp. 197–212, 1996.
[34] T. Takama and K. Kobayashi, "Mearsuring interfacial waves on film flowing down tube inner wall using laser focus displacement meter," *International Journal of Multiphase Flow*, vol. 26, pp. 1493–1507, 2000.
[35] T. Hayat, T. Javed, and M. Sajid, "Analytic solution for MHD rotating flow of a second grade fluid over a shrinking surface," *Physics Letters. A*, vol. 372, no. 18, pp. 3264–3273, 2008.
[36] C. I. Chen, C. K. Chen, and Y. T. Yang, "Nonlinear stability analysis of thin condensate falling film inside a rotating vertical cylinder," *International Journal of Heat and Mass Transfer*, vol. 49, no. 3-4, pp. 707–717, 2006.
[37] C.-I. Hung, C.-K. Chen, and J.-S. Tsai, "Weakly nonlinear stability analysis of condensate film flow down a vertical cylinder," *International Journal of Heat and Mass Transfer*, vol. 39, no. 13, pp. 2821–2829, 1996.
[38] C. K. Chen and M. C. Lin, "Weakly nonlinear hydrodynamic stability of the thin newtonian fluid flowing on a rotating circular disk," *Mathematical Problems in Engineering*, vol. 2009, Article ID 948672, 15 pages, 2009.
[39] W. Eckhaus, *Studies in Nonlinear Stability*, Springer, Berlin, Germany, 1965.
[40] M. V. G. Krishna and S. P. Lin, "Nonlinear stability of a viscous film with respect to three-dimensional side-band disturbances," *Physics of Fluids*, vol. 20, no. 7, pp. 1039–1044, 1977.
[41] V. L. Ginzburg and L. D. Landau, "Theory of superconductivity," *Journal of Experimental and Theoretical Physics*, vol. 20, pp. 1064–1082, 1950.
[42] P. J. Cheng and T. W. Lin, "Surface waves on viscoelastic magnetic fluid film flow down a vertical column," *International Journal of Engineering Science*, vol. 45, no. 11, pp. 905–922, 2007.
[43] C. I. Chen, "Non-linear stability characterization of the thin micropolar liquid film flowing down the inner surface of a rotating vertical cylinder," *Communications in Nonlinear Science and Numerical Simulation*, vol. 12, no. 5, pp. 760–775, 2007.